Arab J Sci Eng (2013) 38:383–393
DOI 10.1007/s13369-012-0437-5

RESEARCH ARTICLE - SPECIAL ISSUE - MECHANICAL ENGINEERING

A Study on Late Intake Valve Closing Miller Cycled Diesel Engine

Guven Gonca · Bahri Sahin · Yasin Ust · Adnan Parlak

Received: 15 March 2012 / Accepted: 25 July 2012 / Published online: 5 December 2012

Abstract NO_x emissions released from diesel engines have much detrimental effects on the environment. Hence, these emissions must be decreased to the limited values described by regulations. One of the effective methods is to adopt Miller cycle to diesel engine in order to improve the performance and to reduce NO_x emissions of a diesel engine. In this study, late inlet valve closing Miller cycle is applied to diesel engine by lowering compression ratio with respect to expansion ratio by closing intake valve 10 and 20 crank angles later than that of standard diesel engine by using zero-dimensional single zone model which was verified with experimental data. The obtained results have been compared with standard diesel engine in terms of performance and NO emissions. The results showed that Miller cycled diesel engine is found more efficient and environmentally friendly with less power output than standard diesel engine.

Keywords Miller cycle · Diesel engine · Engine performance · NO_x emission

G. Gonca · B. Sahin · Y. Ust (✉)
Department of Naval Architecture and Marine Engineering, Yildiz Technical University, Besiktas, 34349 Istanbul, Turkey
e-mail: yust@yildiz.edu.tr

A. Parlak
Department of Marine Engineering Operations, Yildiz Technical University, Besiktas, 34349 Istanbul, Turkey

الخلاصة

إن لانبعاثات غازات أكاسيد النيتروجين من محركات الديزل تأثيرات محددة كبيرة على البيئة. لذلك يجب خفض هذه الانبعاثات إلى القيم المحدودة الموصوفة بالأنظمة. واحدى الطرق الفعالة هي في اعتماد دورة ميلر لمحرك الديزل من أجل تحسين الأداء وتقليل انبعاثات أكاسيد النيتروجين لمحرك الديزل. وقد تم - في هذه الدراسة - تطبيق دورة ميلر ذات صمام إدخال مغلق متأخر (LIVC) في محرك الديزل عن طريق خفض نسبة الضغط بالنسبة إلى نسبة التمدد ، وذلك بإغلاق صمام الامتصاص 10 و زوايا ذراع المحرّك 20 في وقت لاحق من ذلك الذي في محرك الديزل القياسي باستخدام أنموذج الطبقة المفرد عديم البعد الذي تم التثبت منه بالبيانات التجريبية. وتمت مقارنة النتائج المحصول عليها بمحرك الديزل القياسي بالنسبة للأداء و انبعاثات أكاسيد النيتروجين. وأظهرت النتائج أن محرك الديزل بدورة ميلر وجد فعالا أكثر وصديقا للبيئة مع مخرج طاقة أقل من محرك الديزل القياسي.

List of Symbols

A	Heat transfer area (cm^2)
c_p	Constant pressure specific heat (J/g K)
C	Blowby coefficient
B	Bore (cm)
F	Fuel–air ratio
h	Specific enthalpy (J/g)
h_{tr}	Heat transfer coefficient ($W/m^2/K$)
H_u	Lower heating value (J/g)
Δh	Combustion enthalpy of fuel (J)
m	Mass (g)
$\dot{m}$	Time-dependent mass rate (g/s)
M	Molecular weight (g)
n	Injection constant
p	Pressure (bar)
P	Power (kW)
N	Revolution per minute
Q	Loss heat passed through the cylinder wall (J)
$\dot{Q}$	Rate of heat transfer (W)
RGF	Residual gas fraction

S	Stroke (cm)
$\bar{S}_p$	Mean piston velocity (m/s)
T	Temperature (K)
U	Internal energy (J)
v	Specific volume (cm^3/g)
V	Volume (cm^3)
W	Work output (J)
$\dot{x}_i$	Fraction rate of the total injected fuel mass
$\dot{x}_b$	Fraction rate of the total burned fuel mass

Greek Letters

ε	Ratio of half stroke to rod length
ϕ	Equivalence ratio
$\Gamma(n)$	Gama function depending on n
θ	Crank angle ($\circ$)
τ	Time (ms)
ω	Angular velocity (rad/s)
η	Thermal efficiency

Subscripts

1	At the beginning of the compression
a	Air
b	Burning
cyl	Cylinder
di	Injection duration parameter
db	Burning duration parameter
e	Effective
f	Fuel
fi	Injected fuel
fb	Burned fuel
I	Injection, indicated
id	Ignition delay
l	Loss
s	Stroke
si	Start of fuel injection
sb	Start of burning
st	Stoichiometric
tfmep	Total friction mean effective pressure
w	Cylinder walls

1 Introduction

In modern life, diesel engines have a prominent place in land and sea transportations. Because of reduction in fuel resources and environmental reasons, diesel engines running more efficiently and releasing less emission, particularly NO_x emissions, must be designed as other engines using fossil fuel resources. One of the methods proposed to improve the performance and to diminish NO_x emissions is applying Miller cycle to the engines. In some studies, Miller cycle was applied to petrol engines and natural gas engines by comparing with Otto cycle. As a result, NO_x emissions were decreased with little power loss [1–3]. In a theoretical analysis, it is shown that an air-standard Miller cycle taking into account the heat loss as a percentage of fuel's energy, friction and variable specific heats of working fluid was better than Otto cycle, under the restriction of peak temperature of the cycle [4]. Wu et al. [5] analyzed a supercharged Miller cycle Otto engine. In the study, they stated that the Miller cycle Otto engine has more work output and could have less engine knock problem. Kesgin [6] applied the Miller cycle to a V20 two-stage turbocharged natural gas engine. The Miller cycle was performed experimentally and computationally. The efficiency of the engine was increased and NO_x emissions were kept under the limits.

In another experimental study, applying Miller cycle to the diesel engine could reduce the NO_x emission from the diesel engine was shown with early inlet valve closing version [7]. Ge et al. [8] analyzed and compared the reciprocating heat-engine cycles and also showed the performance of the Miller cycle by using numerical examples and they also [9] investigated the effects of friction and heat transfer loss on the performance of an air standard Miller cycle by using finite-time thermodynamics. Al-Sarkhi et al. [10] conducted an analysis of an air standard Miller cycle in terms of thermal efficiency, compression and expansion ratios by expressing the effect of the temperature-dependent specific heat of the working fluid on the irreversible Miller cycle. In another study, they [11] analyzed a Miller engine in terms of different specific heat models and they showed that the cycle performance can be predicted more accurately by using fourth order polynomial model. Uzuneanu and Panait [12] investigated the thermodynamic efficiency of a supercharged Miller cycle. Zhao and Chen [13] studied on an irreversible Miller cycle model considering some irreversibilities in the compression, expansion, finite time processes and heat loss through the cylinder wall. In their study, an optimization was carried out with respect to the pressure ratios. The optimum criteria of the power output, efficiency and pressure ratio were determined. Gonca et al. [14,15] applied the Miller cycle to the diesel engine by using two-zone combustion model and compared the results of conventional diesel and Miller cycled diesel engine.

In the presented study, apart from the given above studies late inlet valve closing (LIVC) Miller cycled diesel engines (Miller-1 and Miller-2 cycles are retarded 10 and 20 crank angles, respectively) have been modeled by using zero-dimensional single zone combustion model because it is simpler and faster in comparison with multi-dimensional models and it was verified with experimental data [21] for standard diesel engine and the model also gives reasonable results for Miller cycled diesel engines. While the earlier theoretical studies related with internal combustion engines are focused on finite time thermodynamics theory and air standard cycle

models, the experimental studies do not contain a theoretical basis on diesel combustion [1–13].

2 Theoretical Model

Thermodynamic simulation of fuel injected engine is carried out by using zero-dimensional single zone combustion model to calculate NO emissions, effective efficiency, specific fuel consumption (SFC) and effective power. In the cylinder, the equation of the energy conservation in differential form may be written as [16]:

$$\frac{\mathrm{d}U}{\mathrm{d}\theta} = \frac{\mathrm{d}Q}{\mathrm{d}\theta} + \frac{\mathrm{d}W_\mathrm{i}}{\mathrm{d}\theta} + \frac{\mathrm{d}m_\mathrm{fb}}{\mathrm{d}\theta}h_\mathrm{f} - \frac{\mathrm{d}m_\mathrm{l}}{\mathrm{d}\theta}h_\mathrm{l} \tag{1}$$

where m_l is the leak mass and m_fb is the mass of burned fuel; h_f and h_l are enthalpy of burned fuel and leak mass, respectively. The mass rate of burned fuel can be expressed as:

$$\frac{\mathrm{d}m_\mathrm{fb}}{\mathrm{d}\theta} = \frac{\dot{m}_\mathrm{fb}}{\omega} \tag{2}$$

where $\dot{m}_\mathrm{fb}$ is the time-dependent burned fuel rate and it can also be expressed as:

$$\dot{m} = \dot{x}_\mathrm{b} m_\mathrm{f} \tag{3}$$

where m_f and $\dot{x}_\mathrm{b}$ are the total mass of the injected fuel and fraction rate of the total burned fuel mass, respectively, which can be given as:

$$m_\mathrm{f} = \phi F_\mathrm{st}(1 - \mathrm{RGF})m_\mathrm{a} \tag{4}$$

$$\dot{x}_\mathrm{b} = \frac{\omega}{\theta_\mathrm{db}\Gamma(n)}\left(\frac{\theta - \theta_\mathrm{sb}}{\theta_\mathrm{db}}\right)^{n-1}\exp\left[\frac{-(\theta - \theta_\mathrm{sb})}{\theta_\mathrm{db}}\right] \tag{5}$$

where $\Gamma(n)$ is the gamma function [16], θ_db is a parameter of burning duration, θ_Sb is the start of burning, RGF is residual gas fraction. The gamma function is derived as:

$$\ln\Gamma(n) = \left(n - \frac{1}{2}\right)\ln(n) - n + \frac{1}{2}\ln(2\pi) + \frac{1}{12n} - \frac{1}{360n^3} + \frac{1}{1{,}260n^5} - \frac{1}{1{,}680n^7} \tag{6}$$

The value of n could be taken for the diesel engine with open chamber as $1 \le n \le 2$ and for close chamber as $3 \le n \le 5$. But exact value is dependent on fuel used and engine design [16].

The enthalpy of burned fuel may be expressed as:

$$h_\mathrm{f} = \Delta h/M_\mathrm{f} + (P_\mathrm{i} - 1.01325)v_\mathrm{f}/10 \tag{7}$$

where Δh, M_f, P_i and v_f are combustion enthalpy, molecular weight, injection pressure and specific volume of the fuel, respectively. The heat passed through the system boundary with respect to crank angle is written as:

$$\frac{\mathrm{d}Q}{\mathrm{d}\theta} = \frac{\dot{Q}_1}{\omega} \tag{8}$$

where ω is angular velocity and the heat loss rate can be obtained as following:

$$\dot{Q}_1 = h_\mathrm{tr}A_\mathrm{cyl}(T - \mathrm{T_w}) \tag{9}$$

Where h_tr, A_cyl, T and T_w are heat transfer coefficient, heat transfer area of the cylinder, the temperatures of the in-cylinder gas zone and cylinder walls, respectively [16]. The heat transfer coefficient (h_tr) is calculated by using Hohenberg's [17] approach and given as below:

$$h_\mathrm{tr} = C_1 V^{-0.06} P^{0.8} T^{-0.4}(\bar{S}_\mathrm{p} + C_2)^{0.8} \tag{10}$$

where $C_1 = 130$, $C_2 = 1.4$ and $\bar{S}_\mathrm{p}$ is mean piston velocity in meters per second, respectively. The time (crank angle)-dependent expression of the indicated work is given as:

$$\frac{\mathrm{d}W_\mathrm{i}}{\mathrm{d}\theta} = -p\frac{\mathrm{d}V}{\mathrm{d}\theta} \tag{11}$$

where p and V are in-cylinder pressure and volume. The change of stroke volume depending on crank angle is:

$$\frac{\mathrm{d}V}{\mathrm{d}\theta} = \frac{\pi}{8}B^2 S\sin\theta\left[1 + \varepsilon\frac{\cos\theta}{(1 - \varepsilon^2\sin^2\theta)^{\frac{1}{2}}}\right] \tag{12}$$

where B, S and ε are bore, stroke of the cylinder and the ratio of half stroke to rod length, respectively. The time (crank angle)-dependent burned gas leaking through the rings is:

$$\frac{\mathrm{d}m_1}{\mathrm{d}\theta} = \frac{Cm}{\omega} \tag{13}$$

where C is blowby coefficient and the mass balance inside the cylinder can be expressed as:

$$m = m_\mathrm{a} + m_\mathrm{fi} \tag{14}$$

where m_a and m_fi are the masses of the air and injected fuel, respectively. If Eq. (9) is written in differential form, it becomes as follows:

$$\frac{\mathrm{d}m}{\mathrm{d}\theta} = \frac{\mathrm{d}m_\mathrm{a}}{\mathrm{d}\theta} + \frac{\mathrm{d}m_\mathrm{fi}}{\mathrm{d}\theta} \tag{15}$$

The air and injected fuel rates changing with crank angle within the cylinder are expressed, respectively, as:

$$\frac{\mathrm{d}m_\mathrm{a}}{\mathrm{d}\theta} = \frac{-\dot{m}_1/\omega}{1 + \phi F_\mathrm{st}} = \frac{-Cm_\mathrm{a}}{\omega} \tag{16}$$

$$\frac{\mathrm{d}m_\mathrm{fi}}{\mathrm{d}\theta} = \frac{1}{\omega}\left(\dot{m}_\mathrm{fi} - \frac{\dot{m}_1\phi F_\mathrm{st}}{1 + \phi F_\mathrm{st}}\right) = \frac{\dot{m}_\mathrm{fi} - Cm_\mathrm{fi}}{\omega} \tag{17}$$

where $\dot{m}$, ϕ and F_st are the time-dependent gas leak rate, the equivalence ratio and the stoichiometric fuel–air ratio,

respectively. $\dot{m}_{\mathrm{fi}}$ is the time-dependent injected fuel rate and it can also be expressed as:

$$\dot{m}_{\mathrm{fi}} = \dot{x}_{\mathrm{i}} m_{\mathrm{f}} \tag{18}$$

where $\dot{x}_{\mathrm{i}}$ is fraction rate of the total injected fuel mass, respectively, which can be given as:

$$\dot{x}_{\mathrm{i}} = \frac{\omega}{\theta_{\mathrm{di}}\Gamma(n)}\left(\frac{\theta-\theta_{\mathrm{si}}}{\theta_{\mathrm{di}}}\right)^{n-1}\exp\left[\frac{-(\theta-\theta_{\mathrm{si}})}{\theta_{\mathrm{di}}}\right] \tag{19}$$

where θ_{di} is a parameter of injection duration, θ_{si} is the start of fuel injection.

Sitkei [18] correlation used to calculate ignition delay is written as follows:

$$\tau_{\mathrm{id}} = 0.5 + 0.1332P^{-0.7}\mathrm{e}^{\frac{3.92782}{T}} + 4.637P^{-1.8}\mathrm{e}^{\frac{3.92782}{T}} \tag{20}$$

where P and T are temperature and pressure during the ignition delay. By substituting Eqs. (2)–(14) into the Eq. (1), the internal energy change can be rewritten as:

$$\begin{aligned}\frac{\mathrm{d}U}{\mathrm{d}\theta} = &-\frac{C_1 V^{-0.06}P^{0.8}T^{-0.4}(\bar{S}_{\mathrm{p}}+C_2)^{0.8}A_{\mathrm{cyl}}(T-T_{\mathrm{w}})}{\omega}\\ &- p\frac{\pi}{8}B^2 S\,\sin\theta\left[1+\varepsilon\frac{\cos\theta}{(1-\varepsilon^2\sin^2\theta)^{\frac{1}{2}}}\right]-\frac{C(m_{\mathrm{a}}+m_{\mathrm{fi}})h_1}{\omega}\\ &+\frac{\frac{\omega}{\theta_{\mathrm{db}}\Gamma(n)}\left(\frac{\theta-\theta_{\mathrm{sb}}}{\theta_{\mathrm{db}}}\right)^{n-1}\exp\left[\frac{-(\theta-\theta_{\mathrm{sb}})}{\theta_{\mathrm{db}}}\right]\phi F_{\mathrm{st}}(1-\mathrm{RGF})m_{\mathrm{a}}(\Delta h/M_{\mathrm{f}}+(p_{\mathrm{i}}-1.01325)v_{\mathrm{f}}/10)}{\omega}\end{aligned} \tag{21}$$

The time (crank angle)-dependent expressions of pressure and mean gas temperature are given, respectively, as:

$$\frac{\mathrm{d}p}{\mathrm{d}\theta} = \frac{-\frac{pV}{T}\left[\frac{10c_{\mathrm{p}}T}{pV}-\frac{\partial\ln v}{\partial\ln T}\right]\frac{\mathrm{d}v}{\mathrm{d}\theta}-\frac{10\frac{\mathrm{d}u}{\mathrm{d}\theta}\frac{\partial\ln v}{\partial\ln T}}{p}}{\frac{V^2}{T}\left[\left(-\frac{10C_{\mathrm{p}}T}{pV}+\frac{\partial\ln v}{\partial\ln T}\right)\left(-\frac{\partial\ln v}{\partial\ln p}\right)+\frac{\partial\ln v}{\partial\ln T}\left(\frac{\partial\ln v}{\partial\ln T}+\frac{\partial\ln v}{\partial\ln p}\right)\right]} \tag{22}$$

$$\frac{\mathrm{d}T}{\mathrm{d}\theta} = \frac{-V\left[\frac{10\left(\frac{\mathrm{d}u}{\mathrm{d}\theta}\right)}{p\frac{\partial\ln v}{\partial\ln p}}+\left(\frac{\mathrm{d}v}{\mathrm{d}\theta}\right)\left(\frac{\partial\ln v}{\partial\ln T}+\frac{\partial\ln v}{\partial\ln p}\right)\right]}{\frac{V^2}{T}\left[\left(-\frac{10C_{\mathrm{p}}T}{pV}+\frac{\partial\ln v}{\partial\ln T}\right)\left(-\frac{\partial\ln v}{\partial\ln p}\right)+\frac{\partial\ln v}{\partial\ln T}\left(\frac{\partial\ln v}{\partial\ln T}+\frac{\partial\ln v}{\partial\ln p}\right)\right]} \tag{23}$$

In order to solve the differential equations given above, the modified RATES and STATE codes are used [16]. The expression of total friction mean effective pressure is stated as [19]:

$$p_{\mathrm{tfmep}} = Z + 48\left(\frac{N}{1{,}000}\right) + 0.4\bar{S}_{\mathrm{p}}^2 \tag{24}$$

where $\bar{S}_{\mathrm{p}}$ is mean piston velocity in meters per second, N is engine speed (rpm) and $Z = 75\,\mathrm{kPa}$. The effective work output is expressed as:

$$W_{\mathrm{e}} = W_{\mathrm{i}} - W_1 \tag{25}$$

and the work of mechanical loss may be given as:

$$W_1 = \frac{P_{\mathrm{tfmep}}V_{\mathrm{s}}}{10} \tag{26}$$

The effective power output and thermal efficiency can be obtained, respectively, as:

$$P_{\mathrm{e}} = \frac{W_{\mathrm{e}}N}{120} \tag{27}$$

and

$$\eta_{\mathrm{e}} = \frac{P_{\mathrm{e}}}{\dot{m}_{\mathrm{f}}H_{\mathrm{u}}} \tag{28}$$

NO emissions are found in terms of reaction kinetics. NO emissions are calculated by using extended Zeldovich mechanism taking into account ten combustion products including (CO_2, H_2O, N_2, O_2, CO, H_2, H, O, OH, NO) [19]. The combustion analysis is performed by using two codes (FARG and ECP) developed by Olikara and Borman [20].

The reaction steps of NO formation can be seen in Table 1 and the rate constant is given as:

$$k = A_{\mathrm{A}}T^{B_{\mathrm{A}}}\mathrm{e}^{\frac{E_{\mathrm{A}}}{T}} \tag{29}$$

The rate of NO formation (mol cm^{-3} s^{-1}) is used as in [19]:

$$\frac{\mathrm{d[NO]}}{\mathrm{d}t} = \frac{2R_1(1-\alpha^2)}{1+\frac{\alpha R_1}{R_2+R_3}} \tag{30}$$

where $\alpha = \frac{[\mathrm{NO}]}{[\mathrm{NO}]_{\mathrm{e}}}$ and $[]_{\mathrm{e}}$ denotes equilibrium concentration. The other constants used in Eq. (30) are

$$R_1 = k_{+1}[\mathrm{N_2}]_{\mathrm{e}}[\mathrm{O_2}]_{\mathrm{e}} = k_{-1}[\mathrm{NO}]_{\mathrm{e}}[\mathrm{N}]_{\mathrm{e}} \tag{31}$$

$$R_2 = k_{+2}[\mathrm{O_2}]_{\mathrm{e}}[\mathrm{N}]_{\mathrm{e}} = k_{-2}[\mathrm{NO}]_{\mathrm{e}}[\mathrm{O}]_{\mathrm{e}} \tag{32}$$

$$R_3 = k_{+3}[\mathrm{OH}]_{\mathrm{e}}[\mathrm{N}]_{\mathrm{e}} = k_{-3}[\mathrm{NO}]_{\mathrm{e}}[\mathrm{H}]_{\mathrm{e}}. \tag{33}$$

3 Results and Discussion

In the study, LIVC Miller cycle is applied to the diesel engine by closing intake valve 10 and 20 crank angles (CA) later than that of conventional diesel engine. Computational study is performed using zero-dimensional single zone combustion model. Inlet valve closing times of 10 CA and 20 CA

Table 1 Reactions of NO formation (3 step)

No.	Reaction	Forward/backward		
		A_A(cm^3/mol s)	B_A	E_A(kcal/mol K)
1	$N_2 + O \leftrightarrow NO + N$	$7.6 \times 10^{13}/1.6 \times 10^{13}$	0/0	−38,000/0
2	$O_2 + N \leftrightarrow NO + O$	$6.4 \times 10^{9}/1.5 \times 10^{9}$	0/0	−3,150/ − 19,500
3	$OH + N \leftrightarrow NO + H$	$4.1 \times 10^{13}/2 \times 10^{14}$	0/0	0/ − 23,650

Table 2 Engine specifications

Engine speed range	1,200–2,400 rpm
B	10 cm
S	10.8 cm
R	17
C	3.6–9
ε	0.15
Δh	−174,000 kJ/kg
M_f	199.15 kg/kmol
P_i	150 bar
v_f	1.189 cm^3/g
θ_{si}	−35
θ_{di}	12–12.14
θ_{db}	10–11
RGF	0.01
The range for ϕ	0.7–0.8
F_{st}	0.06907
n	4
p_1	0.945–1 bar
T_1	325 K
T_W	400 K

Table 3 Variable values of the diesel engine with respect to engine speed

rpm	1,200	1,600	2,000	2,200	2,400
θ_{di}	12.14	12.13	12.3	11.935	12
θ_{db}	10	10	11	11	10
C	3.6	5.4	9	6.1	8.2

are named as Miller-1 cycle and Miller-2 cycle, respectively. A performance analysis has been carried out to investigate effects of applying the Miller cycle on the performance and NO emissions of the diesel engine. The input data for the numerical analysis are given in Table 2. For the numerical study, the values of variables which are adopted for the diesel engine are given in Table 3. These values are determined in compliance with experimental data of [21]. In this study, the assumptions related to the mathematical model used are as follows:

- Charge mixture is homogeneous, at anytime.
- Thermodynamic properties are constant.
- Gas leakage is at constant rate.
- Residual gas, air and fuel form an ideal mixture.

Figures 1 and 2 illustrate the changes of pressure versus crank angle and cylinder volume, respectively. As can be seen from the figures, pressure traces of Miller cycles are less than those of standard diesel engine. This is why less air enters into the cylinder as inlet valves of Miller cycled diesel

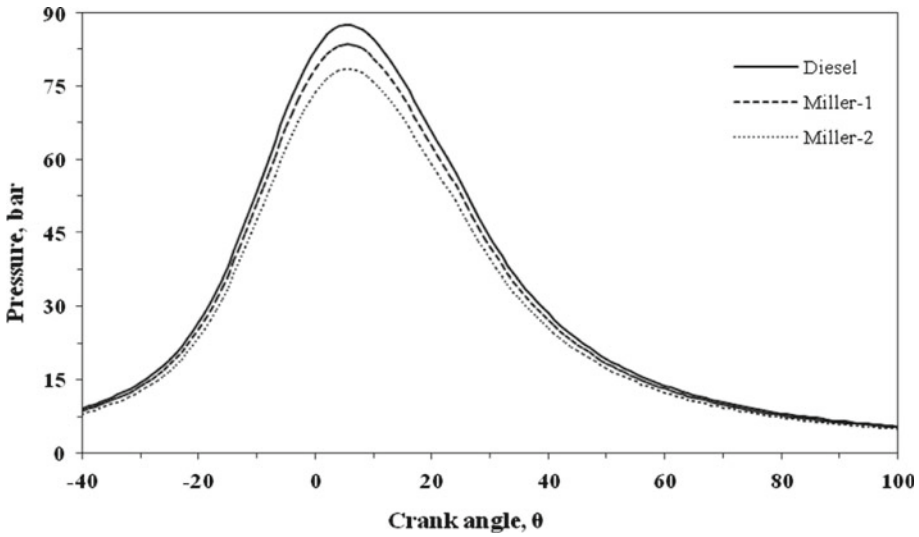

Fig. 1 Comparison of the pressures for various engine modes with respect to crank angle at 2,200 rpm

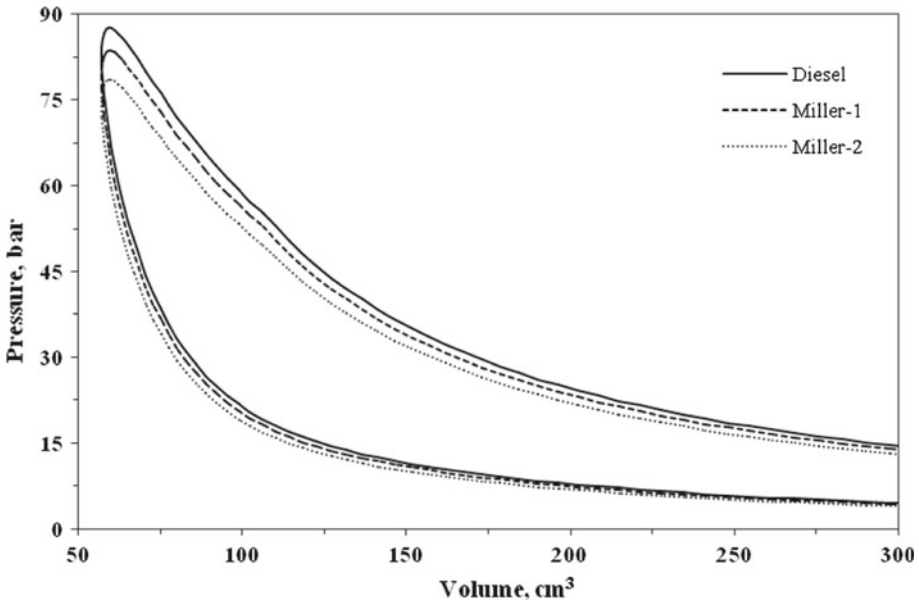

Fig. 2 Comparison of the pressures for various engine modes with respect to cylinder volume at 2,200 rpm

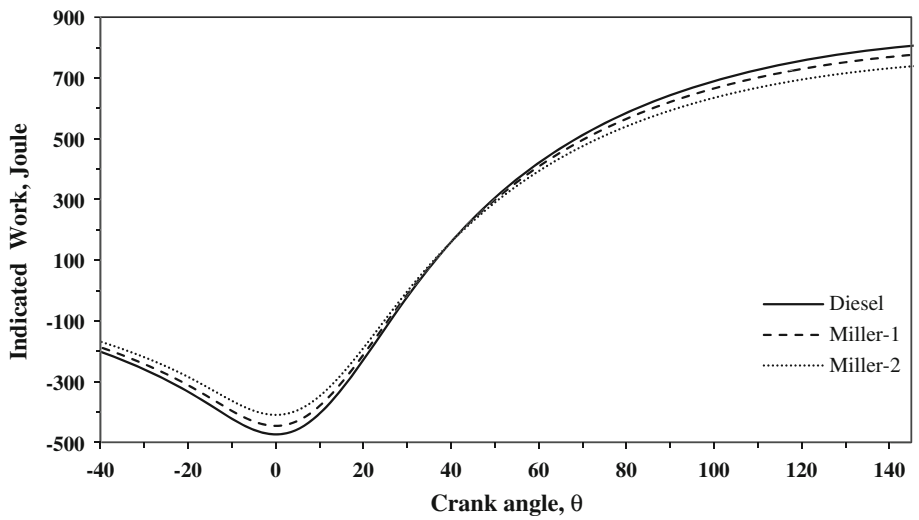

Fig. 3 Comparison of the change of indicated work output for various engine modes with respect to crank angle at 2,200 rpm

engines close later. This leads to lower compression pressure and thus lower peak pressures. Comparing with the diesel cycle, less work is given to the cylinder for the Miller cycles with the decrease of peak pressure and temperature; the indicated works produced by the Miller cycles also decrease as shown in Fig. 3. Effective power of the cycle is also reduced with the decrease of the work output (Fig. 4). The maximum power of Miller cycled diesel engine-1 and 2 are found as 11.7 and 11.8 kW at 2,200 rpm. The reduction rates are 3.0 and 7.2 % in the effective power, respectively. The minimum effective powers are 6.7 and 6.4 kW for Miller cycle-1 and 2, respectively, measured at 1,200 rpm. The reduction rates are 3.3 and 7.7 % in the effective power, respectively. The problem regarding the degradation of performance can be overcome by applying supercharge and optimizing the injection timing, coordinately.

The change of mean gas temperature of diesel engine and Miller cycled diesel engines versus crank angle is depicted in Fig. 5. The Miller cycled diesel engines have lower mean gas temperatures than those of the diesel engine since the peak pressures of Miller cycles are lower. It can be stated that applying the Miller cycle to the diesel engine reduces mean gas temperature with respect to crank angle. However, when the Miller cycle is applied to the diesel engine, effective efficiencies are found higher for both Miller cycle-1 and Miller cycle-2 than those of the standard Diesel engine. Figure 6a, b shows the changes of effective efficiencies and specific SFCs for two modes of Miller cycles depending on the engine speeds. While decreasing mass of injected fuel also decreases effective power but decrease in the rate of mass of injected fuel is more than that of the effective power, the effective efficiency increases and SFC decreases as a result.

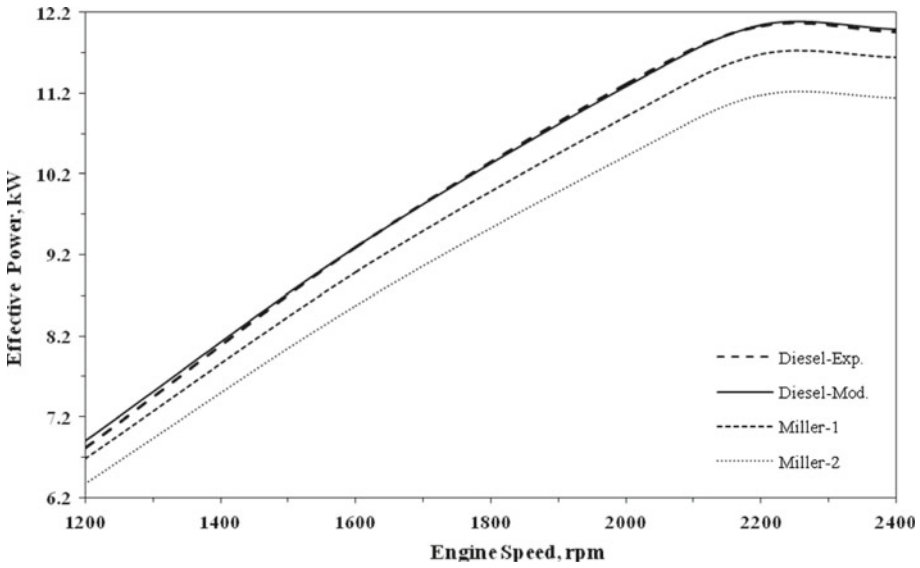

Fig. 4 Comparison of effective powers for various engine modes with respect to engine speed

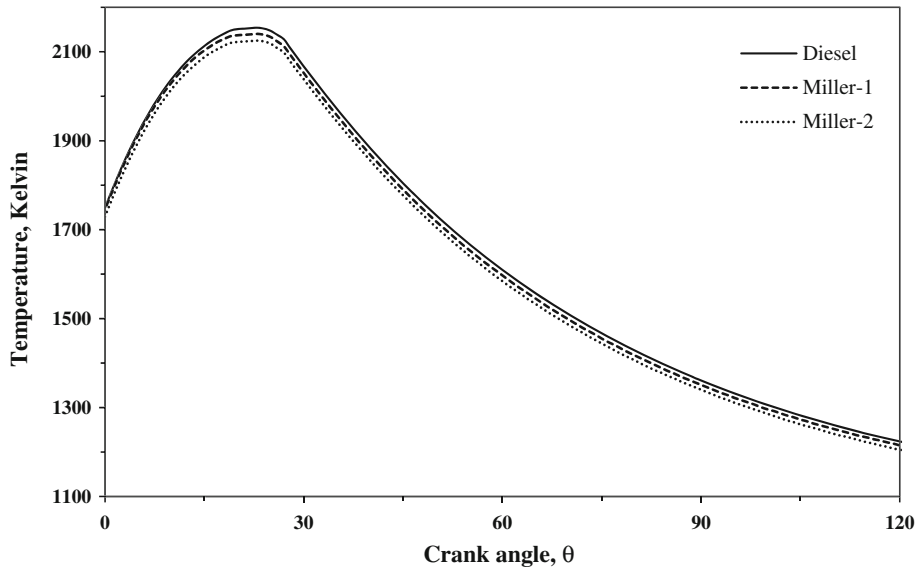

Fig. 5 Comparison of the mean gas temperatures for various engine modes with respect to crank angle at 2,200 rpm

The maximum effective efficiency and minimum SFC of Miller cycled diesel engine-1 and 2 are 29.8 and 30.2 %, 287 and 284 g/kWh at 1,600 rpm, respectively. The amount of improvements in the effective efficiencies and SFC are 1.1 and 2.4 %, respectively. One of the important operating parameters affecting the effective power and efficiency is the equivalence ratio of engine operated. Figure 7 shows the effects of equivalence ratio on the effective power and efficiency for ϕ = 0.7–0.8. The figure shows that the Miller cycled diesel engines maintain less effective power than diesel engine but effective efficiency is higher for the same equivalence ratio. However, the effective power and effective efficiency increase with increasing ϕ. It is clear that applying the Miller cycle reduces peak heat release rates as shown in Fig. 8. The heat release figure shows the reason of higher effective efficiency for Miller cycles is that less fuel is introduced into the cylinder for the same equivalence ratio.

Ignition delay times increase in the cases of Miller cycled diesel engines as the end of compression temperature is less compared to that of standard diesel engine (Fig. 9).

If the amount of air is increased by supercharging and injection timing is retarded according to standard value, it is possible to increase the effective power and efficiency. Figure 10 shows the effects of equivalence ratio on NO formation of the diesel engine and Miller cycled diesel engines. NO formation strongly depends on ϕ. It is known that NO formation rate also depends on in-cylinder temperature with the increase of ϕ and gas temperature is maximum at about $\phi = 1$. Thus, maximum NO formation is obtained with $\phi = 0.8$ whose value is assumed as upper limit of these engines at the

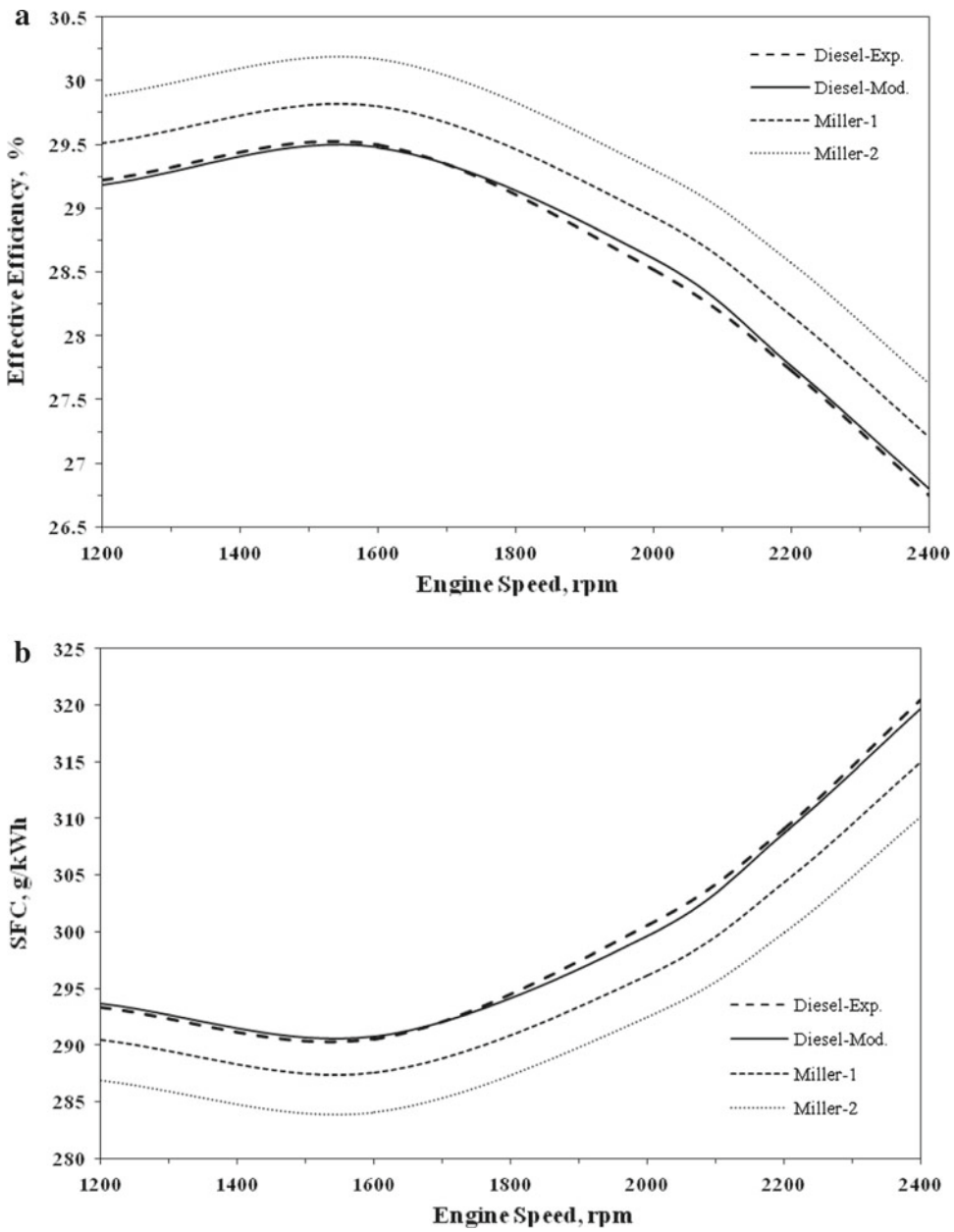

Fig. 6 **a** Comparison of the effective efficiency for various engine modes with respect to engine speed. **b** Comparison of the specific fuel consumption for various engine modes with respect to engine speed

full load condition. NO formation is lower for the two Miller cycle modes for the same ϕ values because less fuel and air are introduced into the cylinder. The main reason of power and gas temperature reduction is that lesser air enters the cylinder in the modes of Miller cycle as inlet valve closes later compared to that of the diesel engine mode. NO formation rate also depends on engine speed as the ϕ changes with engines speed as shown in Fig. 11. There is not only decrease in temperature and pressure but also there is a decrease in the duration of combustion. Combustion temperature, duration of combustion and pressure also affect NO formation rate in this combustion model. When the engine speed increases gas temperature rises as fuel-air ratio closes to stoichiometric ratio and NO also increases. NO reaches a maximum value at maximum temperature. While φ decreases air–fuel mixture becomes leaner which causes to lower temperature and NO formation. For the same ϕ, there is a steady reduction in NO emission released from the Miller cycled diesel engines when compared to diesel engine because of less air and fuel inlet to cylinder. The minimum NO of Miller cycled diesel engines-1 and 2 are 668 and 512 ppm at 1,200 rpm, the reductions in NO emissions are 19.5 and 38.3 %. The maximum NO of Miller cycled diesel engines-1 and 2 are 738 and 573 ppm at 2,200 rpm, the reductions in NO emissions are 18.6 and 36.8 %. The maximum reductions in NO emissions of the Miller cycled diesel engines-1 and 2 are 21.4 and 41.1 % at 2,000 rpm, respectively. In the literature, there is no experimental study related to Miller cycled diesel engines for

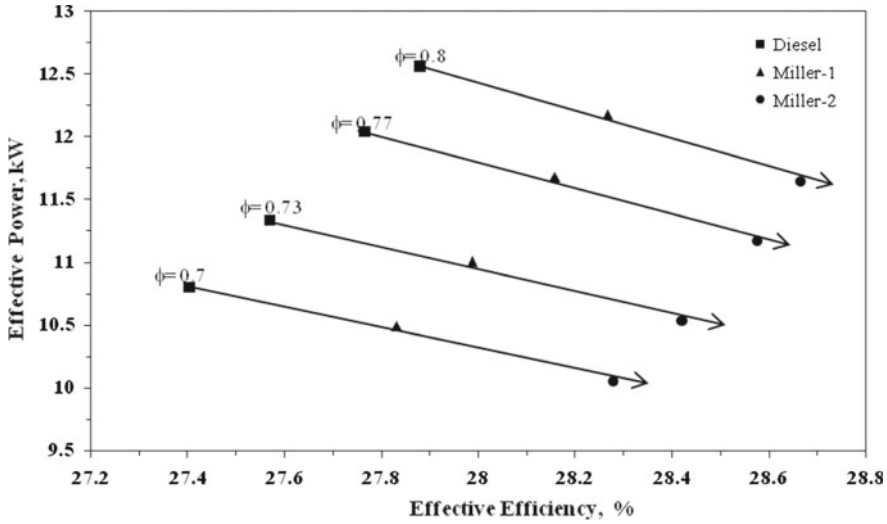

Fig. 7 Comparison of the effective power for various engine modes with respect to effective efficiency at 2,200 rpm

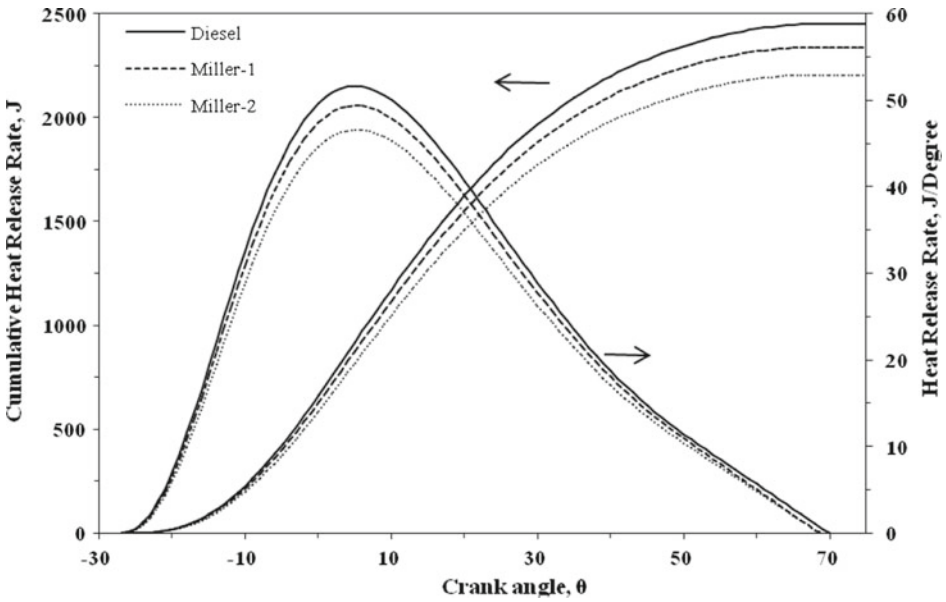

Fig. 8 Comparison of the heat release rates for various engine modes with respect to crank angle at 2,200 rpm

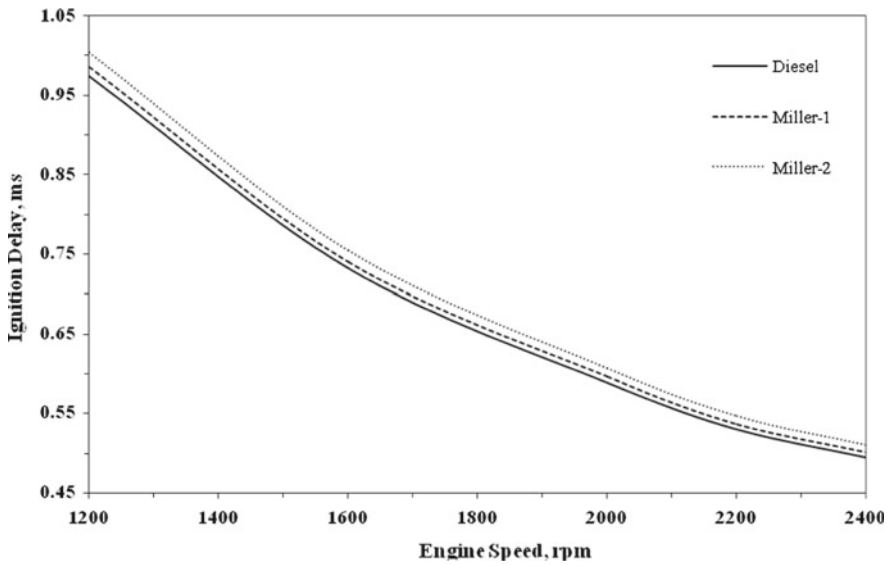

Fig. 9 Comparison of ignition delays for various engine modes with respect to engine speed

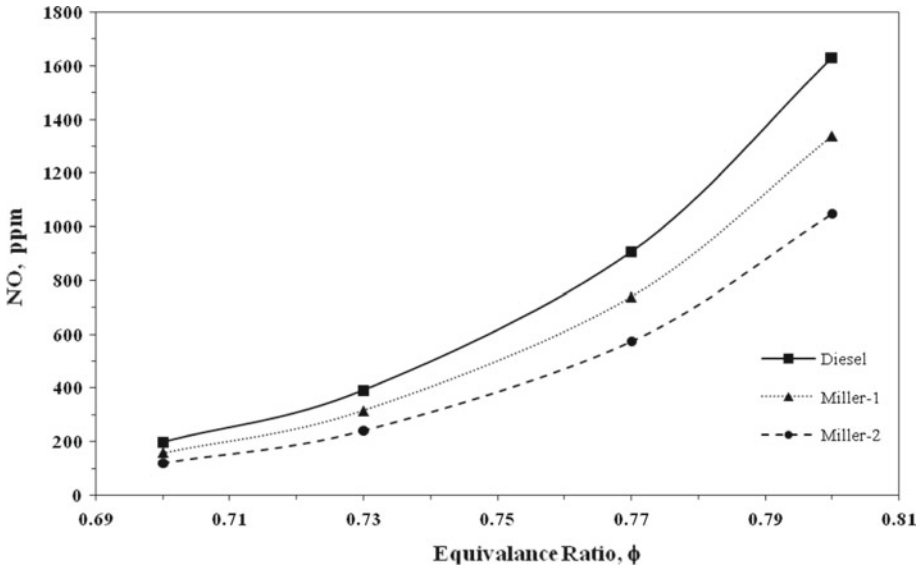

Fig. 10 Comparison of the change of NO for various engine modes with respect to ϕ at 2,200 rpm

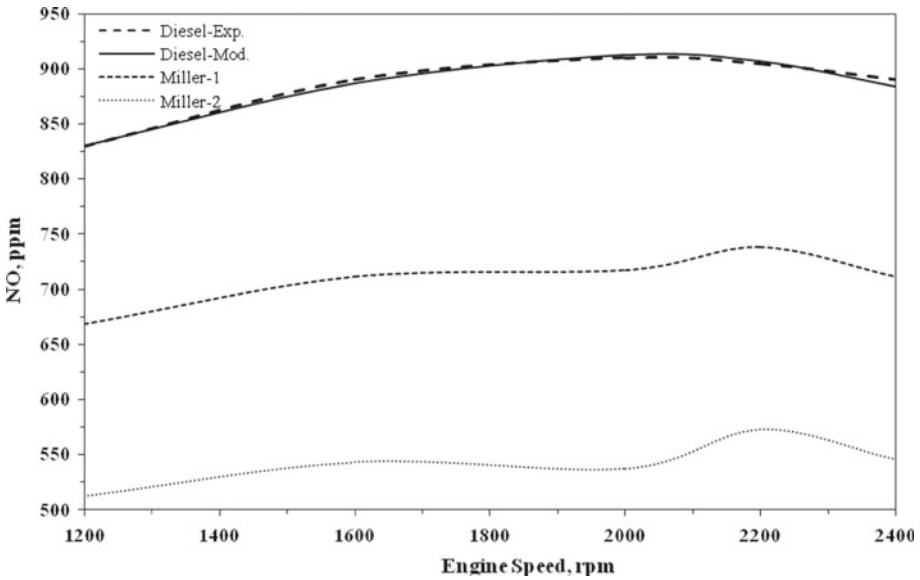

Fig. 11 Comparison of the NO emissions for various engine modes with respect to engine speed

comparison. Thus, the theoretical model which is developed for this study is only compared with the results of experimental data [21] for standard diesel engine. As can be seen from Figs. 4, 6 and 11, the numerical simulations are very close to the experimental data [21] for standard diesel engine. Thus, it is clear that this study presents a good approximation for Miller cycled diesel engines when compared to another study [7].

The engine life depends on how it is used, higher temperatures and pressures shorten the life of the engines and they need maintenance frequently. Noise levels also increase depend on higher temperatures and pressures. In the study, when applying the Miller cycle to diesel engine temperatures and pressures reduce so the engine life is extended, probably Miller cycled Diesel engine has lower noise level.

4 Conclusion

In this study, LIVC Miller cycled diesel engine has been modeled by using zero-dimensional single-zone combustion model. The results have been compared to those of the diesel engine mode. Verification of theoretical model is made with the results of experimental study conducted by Ayhan [21] for a standard diesel engine. The theoretical results closely fit those of the experimental study. It is shown that the model can be applied to Miller cycled diesel engines. When the Miller cycle is applied to the diesel engine, while NO emissions and effective power decreased, the effective efficiency also increased in all the conditions. The reason of power reduction is that lesser air is taken into the cylinder in the modes of Miller cycle as inlet valve closes later compared to that

of the diesel engine mode. For increasing equivalence ratios, the NO emissions, effective power and efficiency increase for both Miller cycles. This study is conducted for the naturally aspirated diesel engines. Supercharging and injection timing optimization can be implemented to the Miller cycled diesel engine for compensating the loss in the power. As a result, it can be said that this method is more environmentally friendly in all conditions but this data must be verified with experimental data for the Miller cycled diesel engines. This study may be used as an approximation in the engineering applications; it could be a leading study for the real-engine designers in the optimization between the performance and NO emission.

Acknowledgments This work has been supported by The Scientific and Technological Research Council of Turkey and was performed within The Support Programme for Scientific and Technological Research Projects (1001) with the project number of 111M056 and given as a part of PhD thesis progress report of the first author.

References

1. Wang, Y.; Lin, L.; Roskilly, A.P.; Zeng, S.; Huang, J., He, Y.; Huang, X.; Huang, H.; Wei, H.; Li, S.; Yang, J.: An analytic study of applying Miller cycle to reduce NO_x emission from petrol engine. Appl. Therm. Eng. **27**, 1779–1789 (2007)
2. Wang, Y.; Lin, L.; Zeng, S.; Huang, J.; Roskilly, A.P.; He, Y.; Huang, X.; Li, S.: An analytic study of applying Miller cycle to reduce NO_x emission from petrol engine. Appl. Energy **85**, 463–474 (2008)
3. Mikalsen, R.; Wang, Y.D.; Roskilly, A.P.: A comparison of Miller and Otto cycle natural gas engines for small scale CHP applications. Appl. Energy **86**, 922–927 (2009)
4. Lin, J.C.; Hou, S.S.: Performance analysis of an air-standard Miller cycle with considerations of heat loss as a percentage of fuel's energy, friction and variable specific heats of working fluid. Int. J. Therm. Sci. **47**, 182–191 (2008)
5. Wu, C.; Puzinauskas, P.V.; Tsai, J.S.: Performance analysis and optimization of a supercharged Miller cycle Otto engine. Appl. Therm. Eng. **23**, 511–521 (2003)
6. Kesgin, U.: Efficiency improvement and NO_x emission reduction potentials of two-stage turbocharged Miller cycle for stationary natural gas engines. Int. J. Energy Res. **29**, 189–216 (1995)
7. Wang, Y.; Zeng, S.; Huang, J.; He, Y.; Huang, X.; Lin, L.; Li, S.: Experimental investigation of applying Miller cycle to reduce NO_x emission from diesel engine. Proc. Inst. Mech. Eng. Part A J. Power Energy **219**, 631–638 (2005)
8. Ge, Y.; Chen, L.; Sun, F.; Wu, C.: Effects of heat transfer and friction on the performance of an irreversible air-standard Miller cycle. Int. Commun. Heat Mass Transf. **32**, 1045–1056 (2005)
9. Ge, Y.; Chen, L.; Sun, F.; Wu, C.: Reciprocating heat-engine cycles. Appl. Energy **81**, 397–408 (2005)
10. Al-Sarkhi, A.; Jaber, J.O.; Probert, S.D.: Efficiency of a Miller engine. Appl. Energy **83**, 343–351 (2006)
11. Al-Sarkhi, A.; Al-Hinti, I.; Abu-Nada, E.; Akash, B.: Performance evaluation of irreversible Miller engine under various specific heat models. Int. Commun. Heat Mass Transf. **34**, 897–906 (2007)
12. Uzuneanu, K.; Panait, T.: Study of the thermodynamic efficiency of a Miller supercharged cycle. Termotehnica **1**, 32–34 (2007). http://www.agir.ro/buletine/596.pdf
13. Zhao, Y.; Chen, J.: Performance analysis of an irreversible Miller heat engine and its optimum criteria. Appl. Therm. Eng. **27**, 2051–2058 (2007)
14. Gonca, G.; Kayadelen, H.K.; Safa, A.; Sahin, B.; Parlak, A.; Ust, Y.: Comparison of diesel engine and Miller cycled diesel engine by using two zone combustion model. 1. In: INTNAM Symposium, vol. 17, pp. 681–697 (2011)
15. Gonca, G.: Investigation of the effects of steam injection into the supercharged diesel engine with running Miller cycle on performance and emissions. PhD thesis progress report (2011)
16. Ferguson, R.: Internal Combustion Engines-Applied Thermodynamic. Wiley, New York (1986)
17. Hohenberg, G.F.: Advanced approaches for heat transfer calculation. SAE Paper No. 790825 (1979)
18. Sitkei, G.: Kraftstoffaufbereitung und Verbrennung bei Dieselmotoren. Springer, Berlin (1964)
19. Heywood, J.B.: Internal Combustion Engines Fundamentals. McGraw Hill Book Company, New York (1989)
20. Olikara, C.; Borman, G.: A computer program for calculating properties of equilibrium combustion products with some applications to the engines. SAE Tech. Papers Series, 750468 (1975)
21. Ayhan, V.: Investigation of the effects of steam injection into the diesel engine on NO_x and PM emissions (in Turkish). Sakarya University PhD thesis (2009)